Gauge singlet scalars as cold dark matter

John McDonald
CFMC-GTAE, Av. Prof. Gama Pinto 2, Lisboa 1699, Portugal
(Received 22 November 1993)

We consider a very simple extension of the standard model in which one or more gauge singlet scalars S_i couples to the standard model via an interaction of the form $\lambda_S S_i^\dagger S_i H^\dagger H$, where H is the standard model Higgs doublet. The thermal relic density of S scalars is calculated as a function of the coupling λ_S and the S scalar mass m_S. The regions of the (m_S,λ_S) parameter space which can be probed by present and future experiments designed to detect scattering of S dark matter particles from Ge nuclei, and to observe upward-moving muons and contained events in neutrino detectors due to high-energy neutrinos from annihilations of S dark matter particles in the Sun and the Earth, are discussed. Present experimental bounds place only very weak constraints on the possibility of thermal relic S scalar dark matter. The next generation of cryogenic Ge detectors and of large area (10^4 m^2) neutrino detectors will be able to investigate most of the parameter space corresponding to thermal relic S scalar dark matter up to $m_S \approx 50$ GeV, while a 1 km^2 detector would in general be able to detect thermal relic S scalar dark matter up to $m_S \approx 100$ GeV and would be able to detect up to $m_S \approx 500$ GeV or more if the Higgs boson is lighter than 100 GeV.

PACS number(s): 95.35.+d, 12.60.Cn

I. INTRODUCTION

There is strong evidence that the mass density of the Universe is mainly composed of some nonhadronic form of dark matter [1,2]. Direct observation of galaxies and clusters of galaxies [2] indicates that $\Omega = 0.1-0.3$, where Ω is the ratio of the mass density to the critical density of the Universe at present. Nucleosynthesis constrains the density of hadronic dark matter to satisfy [3] $0.011 < \Omega_B h^2 < 0.019$, where $h = 0.5-1$ parametrizes the uncertainty in the observed value of the Hubble parameter. Inflation and naturalness considerations [4] suggest that $\Omega = 1$. Although it seems possible that baryons could just about account for $\Omega = 0.1$ dark matter, it would not be possible for primordial density perturbations to grow sufficiently in a baryon-dominated universe to allow galaxy formation [5] to be consistent with the magnitude of temperature fluctuations of the cosmic microwave background radiation as observed by the Cosmic Background Explorer (COBE) [6]. This requires the addition of a density of nonhadronic dark matter, preferably cold dark matter (CDM) [5]. It would also be difficult to explain, if halo dark matter was hadronic in nature, how all the hadrons in galactic halos could be hidden [7]. Searches for faint stars support the conclusion that the halo dark matter cannot primarily be baryonic [8] (although recent observations of microlensing by dark objects in the galactic halo do show that at least some baryonic halo dark matter exists [9]). Thus it is likely that the Universe is dominated by a density of CDM satisfying $\Omega_{\rm CDM} \gtrsim 0.1$. The age of the Universe imposes an upper limit on Ω, $\Omega h^2 \lesssim 1$ [1]. This leaves a window for which a density of particles can consistently serve as the primary component of the halo dark matter, $0.025 \lesssim \Omega h^2 \lesssim 1$.

In this paper we will study in some detail an extremely simple extension of the $SU(3)_c \times SU(2)_L \times U(1)_Y$ standard model, namely, the addition of one or more gauge singlet complex scalars S_i. These scalars, if stable, can in principle account for a density of CDM. Stability of the scalars can most simply be guaranteed if a continuous or discrete symmetry exists under which the gauge singlet scalars are the lightest particles transforming nontrivially. (Additional continuous and discrete symmetries are a common feature of many extensions of the standard model, serving to simplify the models and to eliminate phenomenologically unwelcome interactions such as, those leading to baryon and lepton number violation or to flavor-changing neutral currents.) In addition, it is necessary that the S_i do not acquire vacuum expectation values, which in turn requires that they have positive mass squared terms. This model for CDM is essentially determined by just three parameters: the Higgs boson mass m_h, the S scalar mass m_S, and the coupling of the S scalars to the Higgs bosons λ_S. In particular, we will consider the thermal relic density of S scalars, coming from S scalars freezing out of thermal equilibrium. This is the simplest and most natural origin of a relic density of S scalars, although in principle other possibilities exist, such as S scalars originating from the out-of-equilibrium decay of some heavy particle. We will be particularly interested in the possibility of experimentally detecting S scalar cold dark matter, as a function of λ_S, m_S, and m_h, either via direct detection of the recoil energy coming from elastic scattering of S dark matter particles from Ge nuclei [10,11], or by observing upward-moving muons or contained events in neutrino detectors, produced by high-energy neutrinos coming from S annihilations in the Sun or in the Earth [12–17].

The paper is organized as follows. In Sec. II we discuss the thermal relic density of gauge singlet scalars in the Universe at present. In Sec. III we discuss the elastic

scattering of S scalars from Ge nuclei. In Sec. IV we discuss the rate of upward-moving muons and contained events produced by high-energy neutrinos due to S annihilations in the core of the Sun and the Earth. In Sec. V we give our conclusions. In the Appendix we give some details of calculation of upward-moving muon and contained event rates.

II. S SCALAR DARK MATTER

We consider extending the standard model by the addition of the terms

$$L_S=\partial^\mu S_i^\dagger \partial_\mu S_i - m^2 S_i^\dagger S_i - \lambda_S S_i^\dagger S_i H^\dagger H \ , \tag{2.1}$$

where $i=1,\ldots,N$. This model has a global U(1) symmetry, $S_i \to e^{i\alpha} S_i$, which guarantees the stability of the S_i scalars by eliminating the interaction terms involving odd powers of S_i and $S_i^\dagger$ which lead to S_i decay. We first consider the case $N=1$. In order to calculate the relic density arising from S scalars freezing out of thermal equilibrium, we will use the usual Lee-Weinberg (LW) approximation [18] to solve the rate equation for the density of S scalars. The rate equation is given by

$$\frac{dn_S}{dt} = -3Hn_S - \langle \sigma_{\rm ann} v_{\rm rel} \rangle (n_S^2 - n_0^2) \ . \tag{2.2}$$

$\sigma_{\rm ann}$ is the $SS^\dagger$ annihilation cross section, $v_{\rm rel}$ is the relative velocity of the annihilating particles, and H is the expansion rate of the Universe. The angular brackets denote the thermal average value. (2.2) gives the number density of S scalars n_S. The total density of S and $S^\dagger$ scalars is then $2n_S$. The equilibrium S density n_0, for $m_S/T \gg 1$, is given by

$$n_0 = T^3 \left[\frac{m_S}{2\pi T} \right]^{3/2} e^{-m_S/T} \ . \tag{2.3}$$

The approximate solution of (2.2) is found by rewriting (2.2) as

$$\frac{df}{dT} = \frac{\langle \sigma_{\rm ann} v_{\rm rel} \rangle}{K} (f^2 - f_0^2) \ , \tag{2.4}$$

where $f=n_S/T^3$, $f_0=n_0/T^3$, and $K=[4\pi^3 \bar{g}(T)/45 M_{\rm Pl}^2]^{1/2}$. $\bar{g}(T)$ is the number of degrees of freedom with masses smaller than T. In this we are assuming that the number of degrees of freedom in thermal equilibrium with the photons, $g(T)$, is constant around the S freeze-out temperature T_{fS}, i.e., no particle thresholds at $T \approx T_{fS}$, and also that the Universe is radiation dominated. The LW solution is given by assuming that $f=f_0$ until the temperature at which

$$\left| \frac{df_0}{dT} \right| = \frac{\langle \sigma_{\rm ann} v_{\rm rel} \rangle}{K} f_0^2 \tag{2.5}$$

is satisfied, which defines the S freeze-out temperature T_{fS}. Then for $T < T_{fS}$ one solves (2.4) with $f_0=0$ on the right-hand side and with $f(T_{fS})=f_0(T_{fS})$. The freeze-out temperature is obtained from

$$x_{fS}^{-1} = \ln \left[\frac{m_S x_{fS}^2 A}{(1-3x_{fS}/2)(2\pi x_{fS})^{3/2}} \right] \ , \tag{2.6}$$

where $x_{fS}=T_{fS}/m_S$ and $A=\langle \sigma_{\rm ann} v_{\rm rel} \rangle / K$. The present total mass density in S scalars and antiscalars is then

$$\Omega_S \equiv \frac{\rho_S + \rho_{S\dagger}}{\rho_c} = 2 \frac{g(T_\gamma)}{g(T_{fS})} \frac{K}{T_\gamma x_{fS} \langle \sigma_{\rm ann} v_{\rm rel} \rangle} \times \left[\frac{T_\gamma^4}{\rho_c} \right] \frac{1-3x_{fS}/2}{1-x_{fS}/2} \ , \tag{2.7}$$

where it has been assumed that $\langle \sigma_{\rm ann} v_{\rm rel} \rangle$ is T independent. $\rho_c = 7.5 \times 10^{-47} h^2 \ {\rm GeV}^4$ is the critical closure density of the Universe at present ($h=0.5-11$) and T_γ is the present photon temperature.

In order to calculate $\langle \sigma_{\rm ann} v_{\rm rel} \rangle$ we need the $SS^\dagger$ annihilation modes. These are shown in Fig. 1. The corresponding contributions to $\langle \sigma_{\rm ann} v_{\rm rel} \rangle$ are given by the following.

$SS^\dagger \to h^0 h^0$.

$$\frac{\lambda_S^2}{64\pi m_S^2} \left[1 - \frac{m_h^2}{m_S^2} \right]^{1/2} \ . \tag{2.8a}$$

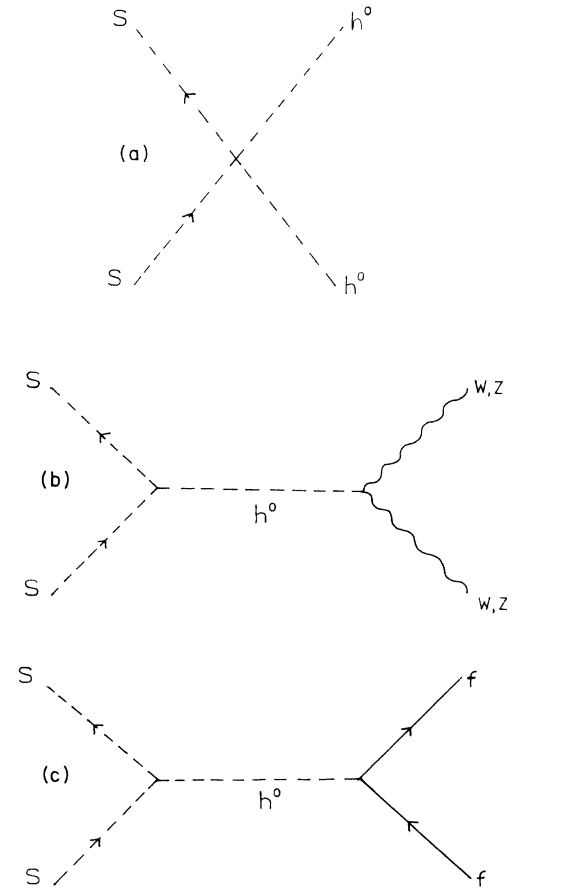

FIG. 1. (a) S annihilation to h^0 pairs. (b) S annihilation to W and Z pairs. (c) S annihilation to fermion pairs.

$SS^\dagger \to W^+W^-$.

$$2\left[1+\frac{1}{2}\left[1-\frac{2m_S^2}{m_W^2}\right]^2\right]\frac{\lambda_S^2 m_W^4}{8\pi m_S^2[(4m_S^2-m_h^2)^2+m_h^2\Gamma_h^2]}\times\left[1-\frac{m_W^2}{m_S^2}\right]^{1/2}. \quad (2.8b)$$

$SS^\dagger \to Z^0Z^0$.

$$2\left[1+\frac{1}{2}\left[1-\frac{2m_S^2}{m_Z^2}\right]^2\right]\frac{\lambda_S^2 m_Z^4}{16\pi m_S^2[(4m_S^2-m_h^2)^2+m_h^2\Gamma_h^2]}\times\left[1-\frac{m_Z^2}{m_S^2}\right]^{1/2}. \quad (2.8c)$$

$SS^\dagger \to \bar{f}f$.

$$\frac{m_W^2}{\pi g^2}\frac{\lambda_f^2\lambda_S^2}{[(4m_S^2-m_h^2)^2+m_h^2\Gamma_h^2]}\left[1-\frac{m_f^2}{m_S^2}\right]^{3/2}. \quad (2.8d)$$

Here the fermion Yukawa coupling is $\lambda_f = m_f/v$, where $v = 250$ GeV and m_f is the fermion mass. m_h is the Higgs boson mass, and Γ_h is the Higgs decay width, for which we use the standard model values [19]. We should note that the assumption made in arriving at (2.7), that $\langle \sigma_{\rm ann} v_{\rm rel} \rangle$ is T independent, is strictly true only for freeze-out temperatures small compared with the electroweak phase transition temperature $T_{\rm EW}$, where [20]

$$T_{\rm EW} = \frac{2.4 m_h}{[1+0.62(m_t/m_W)^2]^{1/2}} \quad (2.9)$$

and m_t is the t quark mass. The thermal expectation value of the Higgs field is given by $\langle h^0 \rangle_T = v(1-T^2/T_{\rm EW}^2)^{1/2}$. Thus for $T_{fS} \gtrsim T_{\rm EW}$ the effective mass of the W and Z bosons goes to zero, while the $\langle h^0 \rangle_T$ -dependent S and h^0 masses differ from their zero temperature values. In practice, however, $T_{fS} \gtrsim T_{\rm EW}$ occurs only for very large S masses $\gtrsim 1$ TeV. In this limit, the S mass is essentially determined by the constant mass term m in (2.1) and so is effectively $\langle h^0 \rangle$ independent, while from (2.8b) and (2.8c), in the limit $m_S \gg m_W$ and $m_S \gg m_h/2$, the contribution from S annihilations to W and Z bosons reduces to three times the contribution from annihilations to the Higgs boson (2.8a), as expected in the SU(2)×U(1) symmetric limit. This is T independent. A large Higgs boson mass does not alter this conclusion, since from (2.9) $T_{\rm EW}$ is of order the Higgs boson mass, and so if T_{fS} is of order $T_{\rm EW}$ then m_S, which, as discussed below, is much larger than T_{fS}, will be much larger than m_h. As a result, we can neglect m_h in the propagators of (2.8). Thus in practice we can use the cross sections (2.8) calculated with the $T=0$ value for $\langle h^0 \rangle$, $\langle h^0 \rangle = 250$ GeV.

Using these contributions to $\langle \sigma_{\rm ann} v_{\rm rel} \rangle$ we solve (2.6) self-consistently for the freeze-out temperature and then obtain from (2.7) the resulting dark matter density. In Figs. 2(a)–2(d) we give plots of the dark matter density as a function of m_S and λ_S for various values of m_h. In these we show the contours for $\Omega_S h^2 = 1.0$, corresponding to the upper limit from the age of the Universe,

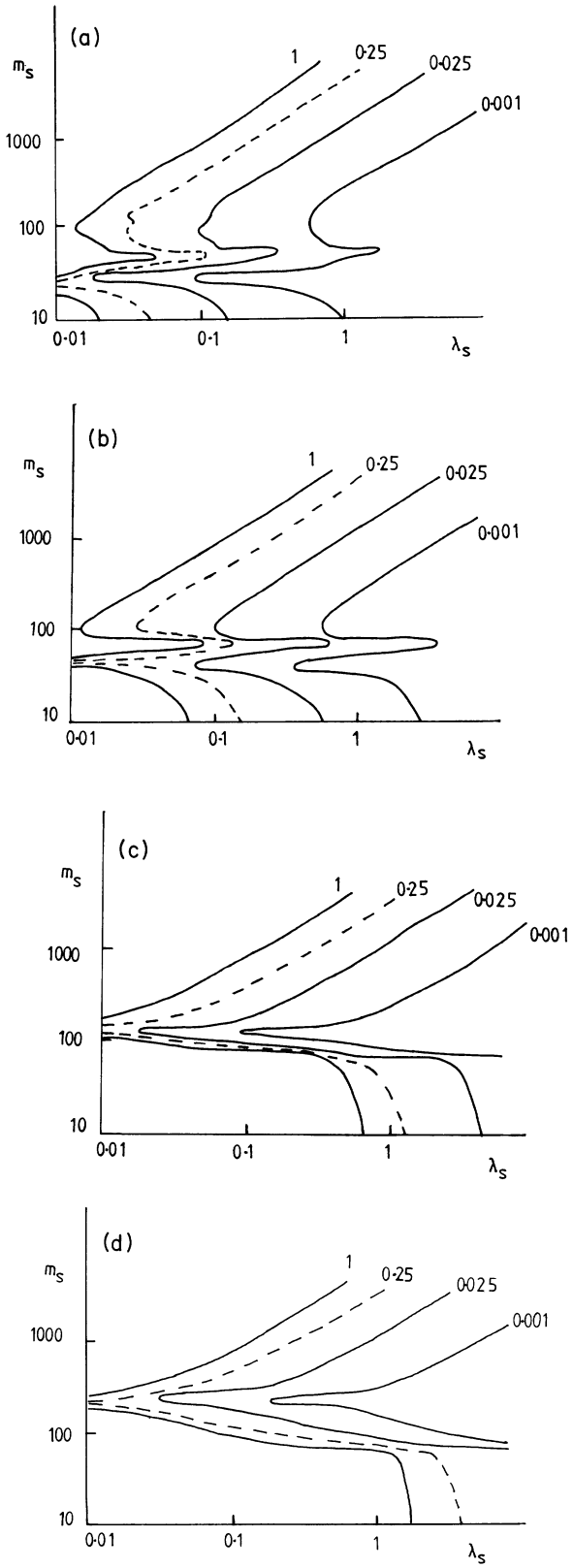

FIG. 2. (a) Thermal relic S scalar density (in units of $\Omega_S h^2$) as a function of λ_S and m_S (in units of GeV) for $m_h = 60$ GeV. (b) Thermal relic S scalar density for $m_h = 100$ GeV. (c) Thermal relic S scalar density for $m_h = 300$ GeV. (d) Thermal relic S scalar density for $m_h = 500$ GeV.

$\Omega_S h^2=0.25$, which is the smallest value for which a critical density ($\Omega_S=1$) of S scalars can occur, and $\Omega_S h^2=0.025$, corresponding to the smallest value for which S dark matter could make up the primary component of the galactic halo. In Table I we give values of the freeze-out temperature for various values of λ_S, m_S, and m_h. Typically $m_S=(10-30)T_{fS}$ for the range of parameters we are considering. We have assumed $m_t=120$ GeV throughout. We find that increasing the t quark mass to 200 GeV makes only a very small difference to our results.

From Figs. 2(a)–2(d) we see that for case of large values of λ_S (larger than 0.1), which is particularly interesting from the point of view of the phenomenology of S scalars, in order to have a density of S scalars which can account for a critical density of dark matter ($\Omega_S h^2 \gtrsim 0.25$), we require the S mass typically to be $\lesssim 100$ GeV or $\gtrsim 500$ GeV. More generally, as the Higgs boson mass increases, the value of λ_S for which S particles of mass less than about 100 GeV can account for halo dark matter ($0.025 \lesssim \Omega_S h^2 \lesssim 1$) increases from about $\lambda_S=0.01-0.1$ for $m_h=60$ GeV to $\lambda_S \gtrsim 1$ for $m_h \gtrsim 300$ GeV. This could be important with respect to the possibility of producing S particles via Higgs decay at future multi-TeV hadron colliders such as the CERN Large Hadron Collider (LHC) [19].

These results are for the case $N=1$. If we consider several scalars of equal mass and coupling strength to the Higgs boson (for example, if the S_i were a multiplet under a global symmetry or even a gauge symmetry with symmetry-breaking scale large compared with m_W), then it is easy to see that the total density in S_i and $S_i^\dagger$ is just the sum over each individual S_i density, since each S_i annihilates only with its own antiparticle. Thus

$$\Omega_{s\,\text{total}} \equiv \sum_i \Omega_{S_i} = N\Omega_S \ . \tag{2.10}$$

Since $\Omega_S \propto 1/\langle \sigma_{\text{ann}} v_{\text{rel}} \rangle \propto 1/\lambda_S^2$, we see that Fig. 2 still holds if we replace λ_S by $\hat{\lambda}_S=\lambda_S/\sqrt{N}$ on the horizontal axis. Thus for a given value of Ω_S and m_S the value of λ_S is increased by $\sqrt{N}$. This will increase the strength of interaction with matter and so the observability of S dark matter for $N>1$.

TABLE I. S freeze-out temperature, $x_{fs}^{-1}=m_S/T_{fS}$.

λ_S	m_S	m_h	x_{fS}^{-1}	λ_S	m_S	m_h	x_{fS}^{-1}
1	30	60	34.5	0.01	30	60	25.5
1	30	100	23.5	0.01	30	100	14.6
1	30	300	18.5	0.01	30	300	9.6
1	30	500	16.5	0.01	30	500	7.7
1	100	60	27.9	0.01	100	60	18.9
1	100	100	28.3	0.01	100	100	19.3
1	100	300	26.5	0.01	100	300	17.5
1	100	500	23.9	0.01	100	500	14.9
1	1000	60	25.1	0.01	1000	60	16.1
1	1000	100	25.1	0.01	1000	100	16.1
1	1000	300	25.1	0.01	1000	300	16.1
1	1000	500	25.2	0.01	1000	500	16.2

III. ELASTIC SCATTERING OF S DARK MATTER PARTICLES FROM NUCLEI AND CONSTRAINTS FROM Ge DETECTORS

In this section we consider the constraints on λ_S and m_S following from direct detection of S dark matter particles via elastic scattering of S scalars from Ge nuclei [10,11]. It will be assumed throughout that S dark matter accounts for the halo dark matter density. Although the simplest possibility for the origin of a relic density of S particles is from S freeze-out, in principle there are other possibilities. For example, if a heavy particle such as a heavy right-handed neutrino N decays to S particles (via the Higgs-mediated process $N \to \nu_L S^\dagger S$ in the case of right-handed neutrinos) at a temperature below the S freeze-out temperature (typically between 1 and 50 GeV for $20 \lesssim m_S \lesssim 1000$ GeV), then the S particles so produced will not return to an equilibrium density and will result in a relic S density different from the thermal relic density. In this case halo dark matter could, in principle, be accounted for by any combination of m_S and λ_S. Thus it is important to consider generally what constraints on the parameters of the model are imposed by experimental observations, as well as to compare the constraints with the thermal relic density as a particular example.

The S scattering cross section from quarks via Higgs exchange gives an effective interaction

$$L_{\text{eff}}=\frac{\lambda_S m_q}{m_h^2} S^\dagger S \bar{q} q \ . \tag{3.1}$$

Using the expression for the nuclear matrix element [16,21]

$$\left\langle N \left| \sum_q m_q \bar{q} q \right| N \right\rangle = (7.62)\tfrac{2}{27} m_N \bar{\psi}_N \psi_N \ ,$$

we see that the effective interaction with a nucleus is given by

$$L_{\text{eff}}=(7.62)\frac{2}{27}\frac{\lambda_S m_N}{m_h^2} S^\dagger S \bar{\psi}_N \psi_N \tag{3.2}$$

and that the cross section for coherent S-nucleus scattering is given by

$$\sigma_{S\text{-}N}=(7.62)^2 \frac{1}{(27\pi)^2}\frac{\pi m_N^4}{(m_S+m_N)^2}\frac{\lambda_S^2}{m_h^4} \ . \tag{3.3}$$

In general $\sigma_{S\text{-}N}$ must be multiplied by a correction factor $\zeta_N(m_S)$, which accounts for the fact that at large enough momentum transfer the scattering ceases to be a coherent scattering with the whole nucleus [14]. We will use a correction factor based on integrating a Gaussian nuclear form factor over the Maxwellian velocity distribution of the halo dark matter particles [14,22]:

$$\zeta_N(m_S)=\frac{0.573}{b}\left[1-\frac{\exp[-b/(1+b)]}{\sqrt{(1+b)}} \times \frac{\text{erf}\{[1/(1+b)]^{1/2}\}}{\text{erf}(1)}\right] , \tag{3.4}$$

where

$$b=\tfrac{8}{9}\bar{v}^2 r_{\text{charge}}^2\frac{m_S^2 m_N^2}{(m_S+m_N)^2}\ , \tag{3.5}$$

$$r_{\text{charge}}=5.1(0.3+0.89A^{1/3})\ \text{GeV}^{-1}\ ,$$

and $\bar{v}=v_{300}\times 300$ km s^{-1} is the halo velocity dispersion of the S particles, which is related to the galactic rotation velocity in the isothermal sphere model, v_{rot}, by $\bar{v}=\sqrt{\frac{3}{2}}v_{\text{rot}}$. For the case of scattering from Ge we find that the full cross section is given by

$$\sigma_{S\text{-Ge}}=5.7\times 10^{-36}\ \text{cm}^{-2}\frac{\zeta_N(m_S)}{[1+m_S/(76\ \text{GeV})]^2}\times\left[\frac{100\ \text{GeV}}{m_h}\right]^4\left[\frac{\lambda_S}{0.1}\right]^2\ , \tag{3.6}$$

where $\zeta_N(m_S)$ is given by (3.4) with

$$b=2.2v_{300}^2/[1+(76\ \text{GeV})/m_S]^2\ .$$

In order to compare with experiments we need to know the rate of interaction of the halo dark matter particles with a detector per kg per day. This is given by (without energy threshold) [23]

$$R=\left[\frac{8}{3\pi}\right]^{1/2}\frac{\eta_v\bar{v}\rho_h\sigma_{S-N}\eta_N(m_S)}{m_S m_N}$$
$$=0.069\rho_{0.4}v_{300}\sigma_{36}^N\left[\frac{100\ \text{GeV}}{m_N}\right]\times\left[\frac{100\ \text{GeV}}{m_S}\right]\text{kg}^{-1}\text{d}^{-1}\ , \tag{3.7}$$

where $\rho_{0.4}$ is the density of S scalars in the halo (ρ_h) in units of 0.4 GeV cm^{-3}, $\eta_v\approx 1.3$ is a correction for the motion of the Sun and the Earth, and σ_{36}^N is the form-factor-corrected S-N cross section in units of 10^{-36} cm^{-2}.

It should be noted that the correction factor $\zeta_N(m_S)$ is not accurate for dark matter particle masses much larger than 100 GeV [22]. However, we will see that the experimental constraints in the present model are most important for S masses less than about 100 GeV, in which case the correction factor (3.4) is accurate to about 10% [22].

In Fig. 3 we show the event rate as a function of m_S and λ_S for the cases $m_h=60$, 100, and 300 GeV. We also show the contours corresponding to the thermal relic S dark matter region of the parameter space, $0.025\lesssim\Omega_S h^2\lesssim 1$ (we have assumed $\rho_{0.4}=v_{300}=1$ throughout).

The present experimental upper bound on R corresponds approximately to 100 kg^{-1}d^{-1} for $m_S\gtrsim 10$ GeV [10,11,24]. In general, present ionization detectors may be able to achieve a sensitivity of about 10 kg^{-1}d^{-1} [24], while in the future cryogenic Ge detectors (such as a proposed (500 g^{73} Ge) + (500 g^{76} Ge) detector [25]) should be able to achieve a sensitivity of 0.1 kg^{-1}d^{-1}. We see from Fig. 3 that in order to constrain the thermal relic S region of parameter space we need an upper bound on R which is less than 100 kg^{-1}d^{-1}. For an upper bound on the cross section of 10 kg^{-1}d^{-1}, we can probe a small region of the thermal relic parameter space corresponding to $\lambda_S\gtrsim 0.06$ and $m_S\lesssim 20$ GeV. In order to significantly constrain the possibility of a critical density of S dark matter, $0.25\lesssim\Omega_S h^2\lesssim 1.0$, we require $R\lesssim 1$ kg^{-1}d^{-1}. $R\lesssim 0.1$ kg^{-1}d^{-1} would allow us to detect or exclude almost all thermal relic S dark matter for $m_S\lesssim 50$ GeV, while $R\lesssim 0.01$ kg^{-1}d^{-1} would detect almost all thermal relic S dark matter possibilities for $m_S\lesssim 100$ GeV. These conclusions for $m_S\lesssim 100$ GeV are essentially independent of m_h, as can be seen by comparing Figs. 3(a), 3(b), and 3(c). For $m_S\gtrsim 100$ GeV, the amount of thermal relic parameter space which can be experimentally searched de-

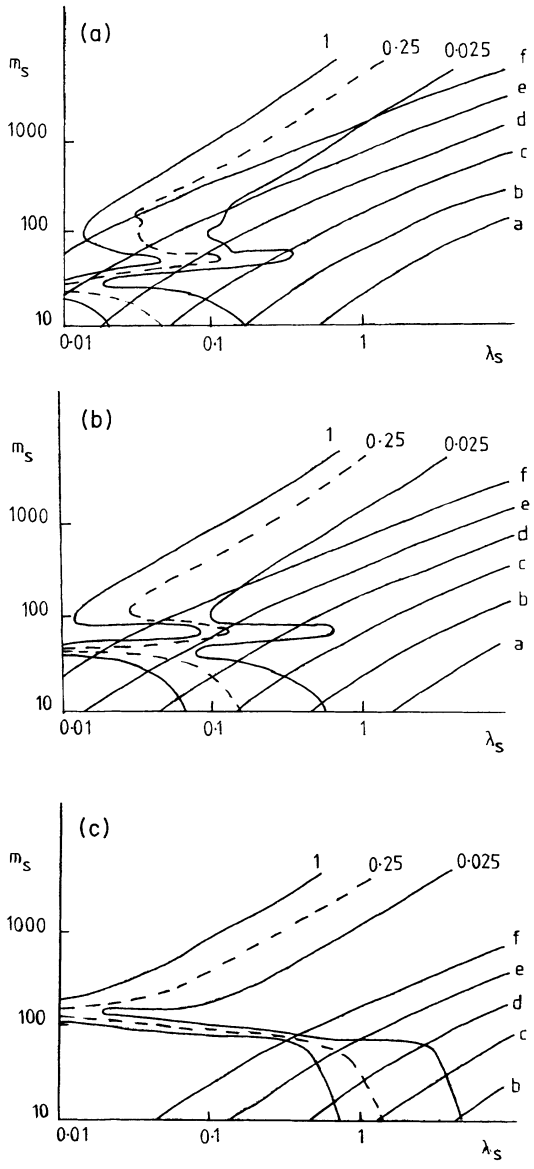

FIG. 3. (a) Ge scattering rate for the case $m_h=60$ GeV. The contours correspond to $R=1000$ kg^{-1}d^{-1} (curve *a*), 100 kg^{-1}d^{-1} (curve *b*), 10 kg^{-1}d^{-1} (curve *c*), 1 kg^{-1}d^{-1} (curve *d*), 0.1 kg^{-1}d^{-1} (curve *e*) and 0.01 kg^{-1}d^{-1} (curve *f*). (b) Ge scattering rate for the case $m_h=100$ GeV. (c) Ge scattering rate for the case $m_h=300$ GeV.

creases as m_h increases. From Fig. 3(a) we see that, even with m_h as small as 60 GeV, in order to constrain thermal relic S halo dark matter for $m_S \gtrsim 100$ GeV we would need $R \lesssim 0.01$ kg^{-1}d^{-1}, and even if an upper bound as low as 0.01 kg^{-1}d^{-1} could be achieved, this would not be sufficient to constrain the possibility of a critical density of thermal relic S dark matter for $m_S \gtrsim 100$ GeV.

Thus we can conclude that since present Ge ionization detectors give an upper bound on R of about 100 kg^{-1}d^{-1} (and are not expected to achieve a sensitivity better than 10 kg^{-1}d^{-1}), present attempts at direct detection of dark matter can at best impose only a very weak constraint on the possibility of thermal relic S dark matter. The next generation of cryogenic detectors should be able to effectively search for S dark matter up to at least 50 GeV. Thermal relic S scalars significantly heavier than 100 GeV are probably beyond the reach of future Ge detectors, even if the Higgs boson mass were as small as 60 GeV.

IV. HIGH-ENERGY NEUTRINOS FROM $SS^\dagger$ ANNIHILATION IN THE EARTH AND IN THE SUN

In this section we calculate the flux of upward-moving muons and the rate of contained events in neutrino detectors due to high-energy neutrinos (>2 GeV) resulting from annihilations of $SS^\dagger$ pairs in the core of the Earth and the Sun [12–17].

The rate of upward-moving muons at the surface of the Earth due to annihilations in the Sun is given by [13]

$$\Gamma_{\text{detector}} = 1.27\times10^{-29} C m_S^2 \times \sum_i a_i b_i \sum_F B_F \langle Nz^2 \rangle_{Fi} \text{ m}^{-2}\text{yr}^{-1} , \quad (4.1)$$

where C is the capture rate in the Sun in units of s^{-1}, a_i and b_i are the neutrino-scattering and muon-range coefficients, summed over $i=\nu_\mu$ and $\bar{\nu}_\mu$ ($a_{\nu_\mu}=6.8$, $a_{\bar{\nu}_\mu}=3.1$, $b_{\nu_\mu}=0.51$, $b_{\bar{\nu}_\mu}=0.67$) and the B_F are the branching ratios for $SS^\dagger$ annihilations to gauge boson, Higgs boson, and quark pairs. $\langle Nz^2 \rangle_{Fi}$ are the second moments of the spectrum of neutrino type i from final state F scaled by the S mass squared:

$$\langle Nz^2 \rangle_{Fi} = \frac{1}{m_S^2} \int \left[\frac{dN}{dE} \right]_{Fi} E^2 dE , \quad (4.2)$$

where $[dN/dE]_{Fi}$ is the differential energy spectrum of neutrino i at the surface of the Sun or Earth resulting from injection of particles in final state F at the center of the Sun or Earth. For the case of annihilations in the Earth one multiplies (4.1) by 5.6×10^8, corresponding to the ratio of the distance squared to the Sun to the radius squared of the Earth [13].

The capture rate is given by [12,14,16,17]

$$C = c \frac{\rho_{0.4}}{m_S v_{300}} \sum_N \sigma_{40}^N F_N(m_S) f_N \phi_N S_N / m_N , \quad (4.3)$$

where σ_{40}^N is the S-nucleus elastic scattering cross section in units of 10^{-40} cm^2. $c = 5.8\times10^{24}$ s^{-1} for the Sun and 5.7×10^{15} s^{-1} for the Earth. The sum is over all species of nuclei N in the Earth or Sun. ϕ_N and f_N are given in Table A.1 of Ref. [17]. S_N is a factor which takes into account the fact that the S dark matter particle must lose sufficient momentum to be captured. For S_N we have

$$S_N \approx (1+A_N^{-1})^{-1} , \quad A_N = \frac{3}{2} \frac{m_S m_N}{(m_S - m_N)^2} \left[\frac{v_{\text{esc}}^2}{\bar{v}^2} \right] \phi_i , \quad (4.4)$$

where v_{esc} is the escape velocity for the Sun or Earth (618 and 11 km s^{-1}, respectively). This has the correct behavior for A_N large and small compared to 1 [14,16]. $F_N(m_S)$ is a factor which takes into account form factor suppression. The branching ratios B_F, corresponding to the rates for S annihilation in the limit of zero relative velocity, are directly obtained from (2.8).

The rate (4.1) assumes that the accretion of S particles by the Sun or Earth and their subsequent annihilation are in equilibrium, in which case the annihilation rate is given by $\Gamma_{\text{ann}} = C/2$. The condition for this to be true is that the age of the solar system $t_\odot$ should be large compared with the time for equilibrium to be established τ_A, which is defined below. In general C in (4.1) should be replaced by [12,16]

$$C \to C \tanh^2 \left[\frac{t_\odot}{\tau_A} \right] , \quad (4.5)$$

where

$$\tau_A = 1/(CC_A)^{1/2} , \quad C_A = \langle \sigma v \rangle V_2 / V_1^2 . \quad (4.6)$$

$\langle \sigma v \rangle$ is the spin-averaged total annihilation cross section times the relative velocity in the limit of zero relative velocity, which can be obtained from (2.8). The effective volumes V_i are given by

$$V_j = 6.5\times10^{28} (j m_S/10 \text{ GeV})^{-3/2} \text{ cm}^3 \quad (4.7a)$$

for the Sun [12] and

$$V_j = 2.0\times10^{25} (j m_S/10 \text{ GeV})^{-3/2} \text{ cm}^3 \quad (4.7b)$$

for the Earth [14].

A second assumption in obtaining (4.1) is that the capture rate is primarily due to single collisions with nuclei ("optically thin" limit). However, for the case of capture due to scattering from iron in the Earth, it has been pointed out that multiple collisions can enhance the capture rate [15]. The enhancement factor is given by

$$\alpha(\tau) = \frac{\exp(\tau_{\text{eff}} - 1)}{\tau_{\text{eff}}} , \quad \tau_{\text{eff}} = \tau\beta_- , \quad (4.8)$$

where

$$\tau \approx \sigma_{S\text{-Fe}} / (2.3\times10^{-33} \text{ cm}^2)$$

is the optical depth of the Earth, $\beta_- = 4 m_S m_{\text{Fe}} / (m_S - m_{\text{Fe}})^2$, and τ_{eff} is the effective optical depth of the Earth taking into account multiple collisions. This expression is valid so long as $\text{Max}(1, \ln\beta_-) \lesssim 6/\tau_{\text{eff}}$ and $\beta_- \lesssim 20$; otherwise the enhancement must be evaluated

numerically, although the largest enhancement occurs typically for $\beta_- \approx 20$ [15]. We have included $\alpha(\tau)$ from (4.8) in our calculations over the range where it is valid (and where enhancement is expected to be most important), in order to indicate the importance or otherwise of multiple collisions. In practice, we find that no enhancement of the event rate in detectors occurs over the range of parameters we are considering.

The $\langle Nz^2 \rangle_{Fi}$ are related to the muon neutrino and antineutrino energy spectra coming from annihilation of S particles in the Sun and Earth, including in the case of the Sun the effects of the interactions of the annihilation products and neutrinos with the solar medium [13]. For $m_S > m_W$ the dominant contributions to the $\langle Nz^2 \rangle_{Fi}$ are from annihilation to gauge boson and t quark final states, while for $m_S < m_W$ the dominant final states contributing to $\langle Nz^2 \rangle_{Fi}$ are b quark pairs and possibly Higgs boson pairs if $m_h < m_W$. In the Appendix we discuss the values of $\langle Nz^2 \rangle_{Fi}$ coming from the different final states.

In order to calculate the capture rate for the case of the Earth one can simply use (4.3), since in this case the form factor suppression is small for most values of m_S [14] and so we can take $F_N(m_S)=1$ [16]. [Capture is dominated by low momentum transfer scattering except for m_S close to the mass of the scattering nucleus, in which case the form factor suppression can be more significant (a factor of 0.72 for the case where $m_S = m_{\mathrm{Fe}}$ [14]).] For the case of capture by the Sun, form factor suppression cannot be neglected, making the calculation of the capture rate more complicated. A simple expression for the capture rate in this case has been given by Kamionkowski [16] which is accurate to 5% for dark matter particle masses greater than a few GeV and less than a few TeV (see also Ref. [14]). In terms of $\sigma_{S\text{-}N}$ this may be written as

$$C = \frac{\pi}{4} \frac{(m_S + m_N)^2}{m_S^2 m_N^4} \sigma_{S\text{-}N} f_S(m_S) , \tag{4.9}$$

where

$$f_S(m_S) = \begin{cases} 2.04\times 10^{38} \exp[-0.0172(m_S - 10)] , & m_S \le 80 \text{ GeV} , \\ 6.10\times 10^{37} (m_S/80)^{-1.06-0.38[(m_S-80)/920]^{1/2}} , & 80 \le m_S \le 1000 \text{ GeV} , \\ 1.72\times 10^{36} (m_S/1000)^{-1.88} , & m_S \ge 1000 \text{ GeV} . \end{cases} \tag{4.10}$$

Here C is in s^{-1} and all masses are in GeV.

In Figs. 4(a)–4(c) we show the results for S annihilations in the Sun for the cases $m_h = 60$, 100, and 300 GeV, respectively, and in Figs. 5(a)–5(c) we show the corresponding results for the case of annihilations in the Earth. Comparing Figs. 4 and 5, we see that for an upper bound on $\Gamma_{\mathrm{detector}}$ corresponding to the IMB upper bound [26], $\Gamma_{\mathrm{detector}} < 2.65\times 10^{-2}\ \mathrm{m}^{-2}\mathrm{yr}^{-1}$ (curve a in Figs. 4 and 5), the strongest constraints on the parameter space come from Earth S annihilations, while for upper bounds less than about $10^{-3}\ \mathrm{m}^2\mathrm{yr}^{-1}$ the solar S annihilations become more important. Thus we will compare the thermal relic parameter space with the Earth S annihilation constraints for the case of the present IMB upper bound and with the solar annihilation S constraints for the case of the bounds expected from future neutrino detectors.

From Fig. 5(a), corresponding to Earth S annihilations with $m_h = 60$ GeV, we see that at present the IMB constraints can probe only a small region of the thermal relic parameter space (corresponding to the iron "resonance" at $m_S \approx 56$ GeV). From Fig. 4(a), we see that for an upper bound on $\Gamma_{\mathrm{detector}}$ of $10^{-3}\ \mathrm{m}^{-2}\mathrm{yr}^{-1}$, upward-moving muons from solar S annihilations can exclude a small region of the thermal relic parameter space corresponding to $\lambda_S \gtrsim 0.1$ and $m_S \lesssim 50$ GeV. [We see from Fig. 5(a) that for this case the bounds due to neutrinos from the Earth are stronger than those due to solar neutrinos for m_S between 20 and 80 GeV, and can probe a significant region of the thermal relic parameter space for m_S between 50 and 70 GeV.] With an upper bound $\Gamma_{\mathrm{detector}} < 10^{-4}\ \mathrm{m}^{-2}\mathrm{yr}^{-1}$, most of the thermal relic parameter space in Fig. 4(a) corresponding to $\Omega_S h^2 \lesssim 0.25$ for $m_S \lesssim 400$ GeV and a significant region of the thermal relic parameter space corresponding to a critical S density for $m_S \lesssim 50$ GeV can be investigated, while an upper bound $\Gamma_{\mathrm{detector}} < 10^{-5}\ \mathrm{m}^{-2}\mathrm{yr}^{-1}$ would probe the whole thermal relic parameter space up to $m_S \approx 500$ GeV. For larger m_h, the conclusions for $m_S \lesssim 100$ GeV are essentially unchanged, while for $m_S \gtrsim 100$ GeV the amount of thermal relic parameter space which can be investigated for a given upper bound on $\Gamma_{\mathrm{detector}}$ decreases as m_h increases.

In order to see how the IMB upper bound could be improved in the future, we can make a rough estimate of the bound which could be imposed by building neutrino detectors of larger area. The IMB bounds follow from a detector area of 400 m^2 and exposure of about 1 yr, corresponding to an upper bound of less than about 10 upward-moving muons per year. Following Ref. [27], we can estimate the area of detector required in order to achieve a given sensitivity by the area needed to detect one upward-moving muon event per year. At present the Monopole, Astrophysics, and Cosmic Ray Observatory (MACRO) detector at Gran Sasso, with an area $\approx 10^3\ \mathrm{m}^2$, is beginning operation [28], while a number of detectors with an effective area of order $10^4\ \mathrm{m}^2$ are under development [Deep Underground Muon and Neutrino Detector (DUMAND) [29], Antarctic Muon and Neutrino Detector Array (AMANDA) [30], the photomultiplier array NESTOR [31]]. In addition, it has been suggested [27]

that a 1 km^2 detector is needed to observe muons from neutralino dark matter in the GeV–TeV mass range, and that this could be constructed at a cost of order 100 million U.S. dollars [32]. We see from Fig. 4 that a detector of area 10^4 m^2 should be able to probe the region of parameter space corresponding to curve *c*, which will rule out much of the parameter space corresponding to thermal relic S dark matter with $m_S \lesssim 50$ GeV. This conclusion is essentially independent of m_h, as can be seen by comparing Figs. 4(a), 4(b), and 4(c). For the case of a 1 km^2 detector, the area of parameter space under curve *e* in Fig. 4 could in principle be searched. This would probe the entire thermal relic dark matter region for $m_S \lesssim 1.5$ TeV (500 GeV, 100 GeV) for the case of $m_h = 60$ GeV (100 GeV, 300 GeV). Thus in general the thermal relic dark matter parameter space can be probed for m_S at least up to 100 GeV.

We therefore conclude that at present the IMB upper bound on the flux of upward-moving muons can impose only a slight constraint on the possibility of thermal relic

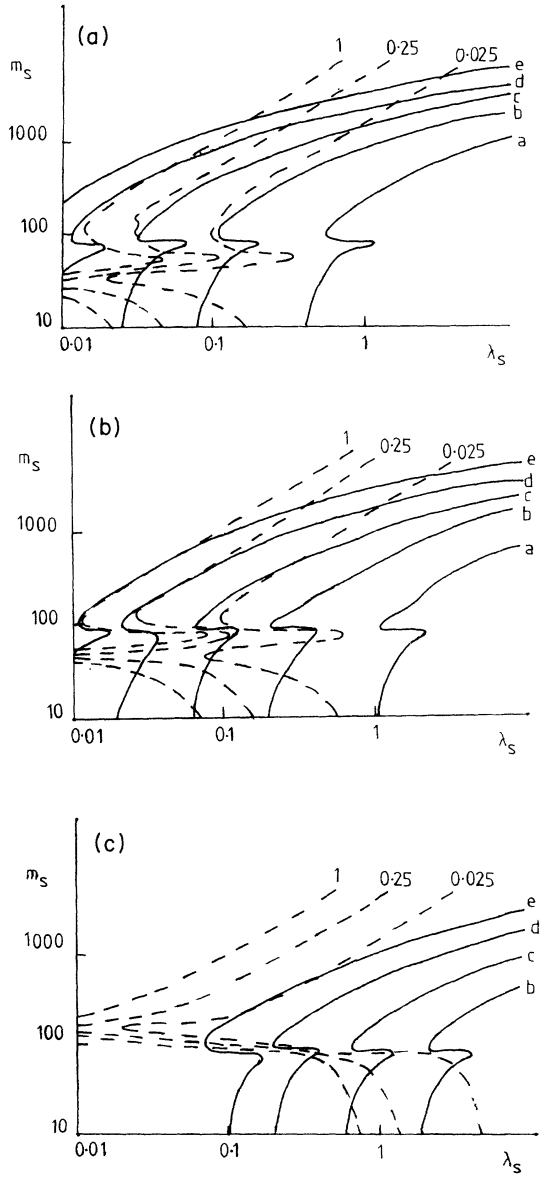

FIG. 4. (a) Rate of upward-moving muons at the Earth's surface due to neutrinos from S annihilation in the Sun, for the case $m_h = 60$ GeV. The contours correspond to $\Gamma_{\text{detector}} = 2.65 \times 10^{-2}$ m^{-1} yr^{-1} (curve *a*), 10^{-3} m^{-2} yr^{-1} (curve b), 10^{-4} m^2 yr^{-1} (curve *c*), 10^{-5} m^{-2} yr^{-1} (curve *d*), and 10^{-6} m^{-2} yr^{-1} (curve *e*). (b) Rate of upward-moving muons at the Earth's surface due to neutrinos from S annihilation in the Sun, for the case $m_h = 100$ GeV. (c) Rate of upward-moving muons at the Earth's surface due to neutrinos from S annihilation in the Sun, for the case $m_h = 300$ GeV.

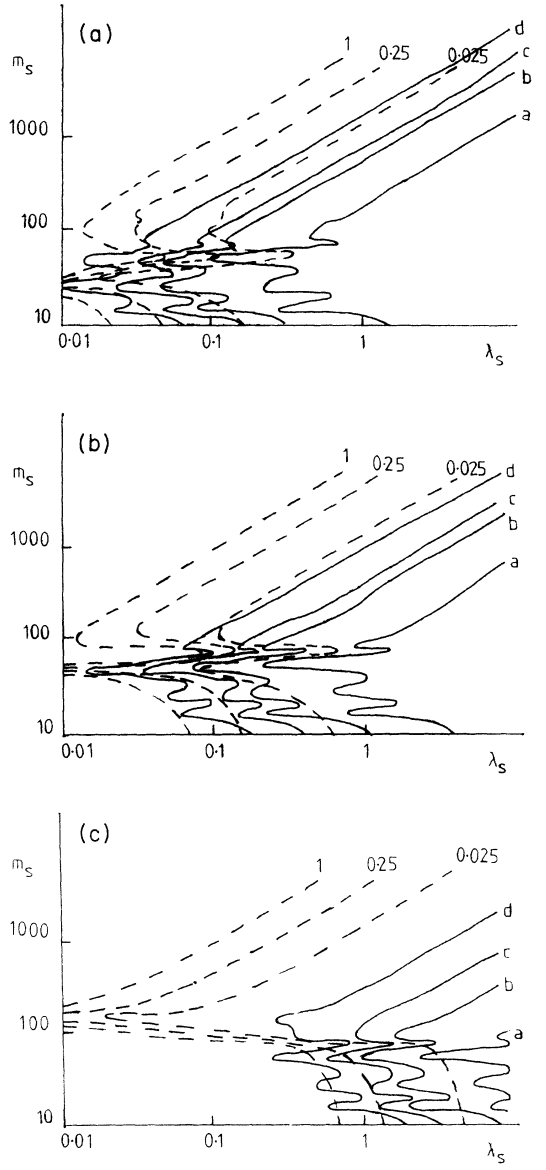

FIG. 5. (a) Rate of upward-moving muons at the Earth's surface due to neutrinos from S annihilation in the Earth, for the case $m_h = 60$ GeV. The contours correspond to $\Gamma_{\text{detector}} = 2.65 \times 10^{-2}$ m^{-2} yr^{-1} (curve *a*), 10^{-3} m^{-2} yr^{-1} (curve *b*), 10^{-4} m^{-2} yr^{-1} (curve *c*), and 10^{-6} m^{-2} yr^{-1} (curve *d*). (b) Rate of upward-moving muons at the Earth's surface due to neutrinos from S annihilation in the Earth, for the case $m_h = 100$ GeV. (c) Rate of upward-moving muons at the Earth's surface due to neutrinos from S annihilation in the Earth, for the case $m_h = 300$ GeV.

S dark matter, while many of the S dark matter possibilities with $m_S \lesssim 50$ GeV should be within the reach of neutrino detectors of area $\sim 10^4$ m^2 in the not-too-distant future. In the more distant future, large (1 km^2) detectors should be able to detect or exclude S dark matter for m_S up to at least 100 GeV.

We also note that in comparing the next generation of Ge detectors, which might reach scattering rates 0.1 kg^{-1} d^{-1} (Fig. 3, curve *e*), with the next generation of neutrino detectors, which might reach upward-moving muon rates 10^{-4} m^2 yr^{-1} (Fig. 4, curve *c*), we find that for $m_S \gtrsim 80$ GeV the constraints from upward-moving muons are dominant, while for $m_S \lesssim 80$ GeV Ge detectors impose stronger constraints.

Up to now we have only considered the rate of upward-moving muons in discussing constraints on the (λ_S, m_S) parameter space. The upward-moving muon flux is the most important signal for high-energy neutrinos from the point of view of future large area neutrino detectors, which are specifically designed to detect this flux. However, in discussing the present bounds on the flux of high-energy neutrinos due to $SS^\dagger$ annihilations, we should also consider the possibility that a high-energy electron or muon neutrino could undergo a charged current interaction within the volume of the detector [13] ("contained event"). For the case of neutrinos from the Sun the rate of contained events per kiloton due to electron and muon neutrinos is given by [13]

$$\Gamma_{\text{detector}} = 3.3\times 10^{-27} C m_S \times \sum_i a_i \sum_F B_F \langle Nz \rangle_{Fi} \text{ kton}^{-1}\,\text{yr}^{-1}, \quad (4.11)$$

where i is summed over the electron and muon neutrino and antineutrino. In the Appendix we discuss the values of $\langle Nz \rangle_{Fi}$ coming from the various final states. In Fig. 6 we show the results for S annihilations in the Sun for the cases $m_h = 60$, 100, and 300 GeV, while in Fig. 7 we show the corresponding results for the case of S annihilations in the Earth. The present upper bound on the rate of electron and muon contained events in the Frejus detector is [17,33] $\Gamma_{\text{detector}} < 6.4$ kton^{-1} yr^{-1}, corresponding to curve *a* in Figs. 6 and 7. Comparing with the upward-moving muon bounds from Figs. 4 and 5, we see that at present the contained event rate imposes constraints on the parameter space which are in general weaker than those coming from the upward-moving muon flux, except at small m_S, $m_S \lesssim 20$ GeV, where the constraints become similar (and slightly stronger for the case of solar neutrinos).

So far in this section and in the previous section, we have considered the case of just one S scalar. For the case of N scalars of equal mass and coupling, the density of each scalar S_i contributes a proportion $1/N$ of the total halo density. The capture rate of S dark matter in the

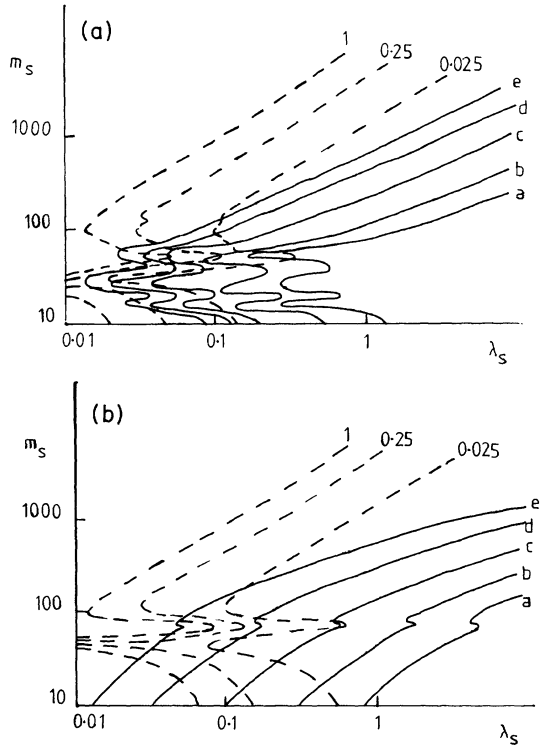

FIG. 6. (a) Rate of contained events due to neutrinos from S annihilation in the Sun, for the case $m_h = 60$ GeV. The contours correspond to $\Gamma_{\text{detector}} = 6.4$ kton^{-1} yr^{-1} (curve *a*), 1 kton^{-1} yr^{-2} (curve *b*), 0.1 kton^{-1} yr^{-1} (curve *c*), 10^{-2} kton^{-1} yr^{-1} (curve *d*), and 10^{-3} kton^{-1} yr^{-1} (curve *e*). (b) Rate of contained events due to neutrinos from S annihilation in the Sun, for the case $m_h = 100$ GeV.

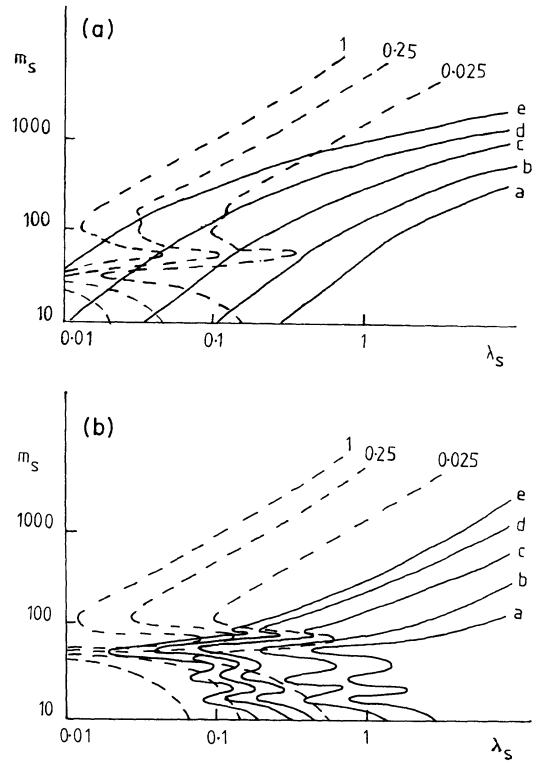

FIG. 7. (a) Rate of contained events due to neutrinos from S annihilation in the Earth, for the case $m_h = 60$ GeV. The contours correspond to $\Gamma_{\text{detector}} = 6.4$ kton^{-1} yr^{-1} (curve *a*), 1 kton^{-1} yr^{-1} (curve *b*), 0.1 kton^{-1} yr^{-1} (curve *c*), 10^{-2} kton^{-1} yr^{-1} (curve *d*), and 10^{-3} kton^{-1} yr^{-1} (curve *e*). (b) Rate of contained events due to neutrinos from S annihilation in the Earth, for the case $m_h = 100$ GeV.

Sun and the Earth and the rate of elastic scattering in Ge detectors are proportional to the density of S_i in the halo times the cross section for scattering from nuclei in the detector or in the Sun or Earth. Thus the contribution to the event rate in a detector is reduced by a factor $1/N$ for a given S_i. The total rate from summing over i for a given m_S and λ_S is therefore unchanged. However, for a given value of the thermal relic density, the value of λ_S for a given m_S is increased by a factor $\sqrt{N}$, leading to an increase in the scattering cross section and so to an increase in the event rate in Ge detectors and in neutrino detectors by a factor N for a given thermal relic density, thus making the dark matter easier to detect.

V. CONCLUSIONS

The extension of the standard model by the addition of a gauge singlet scalar provides a canonically minimal extension of the standard model which can potentially account for dark matter. It is important, therefore, to consider in some detail the question of the relic density of the gauge singlet scalars and their possible observable signatures. In general, present experiments based on observing elastic scattering of halo dark matter particles from Ge nuclei, and on observing upward-moving muons at the Earth's surface, coming from muon neutrinos due to dark matter particle annihilation in the Sun or the Earth, can only place very weak constraints on thermal relic S dark matter, and cannot constrain the possibility that thermal relic S dark matter could account for a critical density of dark mater ($\Omega_S=1$). However, the next generation of cryogenic Ge detectors (which hopefully should achieve bounds on the Ge scattering rate of 0.1 $\text{kg}^{-1}\,\text{d}^{-1}$) and neutrino detectors (with an effective area 10^4 m^2) will be able to investigate most of the parameter space for thermal relic S scalar dark matter with $m_S \lesssim 50$ GeV, while a 1 km^2 neutrino detector, as suggested in order to search for heavy neutralino dark matter, would be able to detect or exclude thermal relic S dark matter for $m_S \lesssim 100$ GeV (as would a cryogenic Ge detector if it could achieve a sensitivity of 0.01 $\text{kg}^{-1}\,\text{d}^{-1}$). For a light Higgs boson mass, equal to 60 GeV (100 GeV), a 1 km^2 detector could also detect heavier thermal relic S dark matter up to 1.5 TeV (500 GeV). In general, the next generation of cryogenic detectors will be the most effective in searching for S dark matter with $m_S \lesssim 80$ GeV, while for $m_S \gtrsim 80$ GeV the next generation of neutrino detectors will be the most effective.

The coupling of a gauge singlet scalar to the standard model Higgs doublet is unique in form and inevitably will be a feature of many particle physics models beyond the standard model. We believe the results presented here may generally be useful in the study of such models and of their cosmological consequences.

ACKNOWLEDGMENTS

This research was funded by the Grupo Teorico de Altas Energias (GTAE), Portugal.

APPENDIX: $\langle Nz^2\rangle_{Fi}$ AND $\langle Nz\rangle_{Fi}$ FROM $SS^\dagger$ ANNIHILATIONS

In this Appendix we give the dominant contributions to $\langle Nz^2\rangle_{Fi}$ and $\langle Nz\rangle_{Fi}$ for the gauge boson, Higgs boson, and quark final states coming from $SS^\dagger$ annihilations. We will use the discussion of Ritz and Seckel [13] (RS) for the case of the quark final states, while for the case of the gauge boson final states we will follow Ref. [16] and consider $\langle Nz^2\rangle_{Fi}$ and $\langle Nz\rangle_{Fi}$ to mostly originate from the highest-energy "semiprompt" W and Z decays to neutrinos. For the case of the Higgs boson final state we will adapt the results of RS to obtain $\langle Nz^2\rangle_{Fi}$ and $\langle Nz\rangle_{Fi}$.

$SS^\dagger \to WW, ZZ$

In this case the dominant contribution to $\langle Nz^2\rangle_{F\nu_\mu}$ comes from muon neutrinos originating in the decays $W^+\to\mu^+\nu_\mu$ and $Z^0\to\nu_\mu\bar{\nu}_\mu$. The mean energy squared of the neutrinos is given by $(m_S^2/4)(1+\beta^2/3)$, where β is the velocity of the decaying W or Z [16] [$\beta=(1-m_W^2/m_S^2)^{1/2}$ for the case of the W]. This assumes that in the rest frame of the W, the W decays isotropically to final states each of energy $m_W/2$. The branching ratio of W^+ to ν_μ decays is given by 1 divided by the number of SU(2) doublets to which W can decay, which gives $\frac{1}{9}$ for W decaying to all lepton doublets and first and second generation quark doublets. Thus, noting that N is the number of neutrinos produced per injected boson or fermion pair [13], we see that the $\langle Nz^2\rangle_{Fi}$ following from annihilation to W pairs can be estimated to be

$$\langle Nz^2\rangle_{W\nu_\mu}\approx\tfrac{1}{9}\tfrac{1}{4}(1+\beta^2/3)=0.028(1+\beta^2/3)\,. \tag{A1}$$

For the case of annihilation to Z pairs, the branching ratio for $Z\to\bar{\nu}_\mu\nu_\mu$ is 0.066 [19], and so the $\langle Nz^2\rangle_{Fi}$ can be estimated to be

$$\langle Nz^2\rangle_{Z\nu_\mu}\approx 2(0.066)\tfrac{1}{4}(1+\beta^2/3)=0.033(1+\beta^2/3)\,, \tag{A2}$$

where the factor 2 occurs because either of the Z's produced by S annihilation can lead to a ν_μ. The same results are obtained for $i=\bar{\nu}_\mu$. For the case of the $\langle Nz\rangle_{Fi}$ one obtains in the same way, for $i=e$ and μ,

$$\langle Nz\rangle_{W\nu_i}\approx\tfrac{1}{9}\tfrac{1}{2}=0.056 \tag{A3}$$

and

$$\langle Nz\rangle_{Z\nu_i}\approx 2(0.066)\tfrac{1}{2}=0.066\,, \tag{A4}$$

where we have replaced the mean energy squared of the neutrinos $(m_S^2/4)(1+\beta^2/3)$ in (A1) and (A2) by the mean energy in the rest frame $m_S/2$. The values of the $\langle Nz\rangle_{Fi}$ for $\bar{\nu}_i$ are equal to those for ν_i.

These results are true for the case where interactions of the W, Z, and neutrinos with the Sun and the Earth are ignored. This is justified for the Earth, but for the case of the Sun there is an additional suppression factor due to the absorption of neutrinos (due to charged current interactions) and loss of neutrino energy (due to neutral

current interactions) as the neutrinos pass through the Sun [13]. (The W and Z will decay fast enough that the effect of their interaction with the solar medium prior to their decay can be ignored [13].) In general the suppression factors are given by [13]

$$P_i = 1/(1+E_0\tau_i)^{n+\alpha_i} , \tag{A5}$$

where E_0 is the initial neutrino energy and $n=2$ (1) for the case of $\langle Nz^2\rangle_{Fi}$ ($\langle Nz\rangle_{Fi}$). $\alpha_{\nu_i}=5.1$, $\alpha_{\bar{\nu}_i}=9.0$, $\tau_{\nu_i}=1.01\times10^{-3}$ GeV^{-1}, and $\tau_{\bar{\nu}_i}=3.8\times10^{-4}$ GeV^{-1} for $i=e,\mu$. The unsuppressed $\langle Nz^2\rangle_{Fi}$ and $\langle Nz\rangle_{Fi}$ are multiplied by the P_i in order to obtain the true $\langle Nz^2\rangle_{Fi}$ and $\langle Nz\rangle_{Fi}$ for the case of neutrinos from the Sun.

It is important to note that the assumption that the $\langle Nz^2\rangle_{Fi}$ and $\langle Nz\rangle_{Fi}$ are dominated by the "semiprompt" decays of the W and Z is well justified for the case of the unsuppressed $\langle Nz^2\rangle_{Fi}$ and $\langle Nz\rangle_{Fi}$ [16], which is appropriate for the case of neutrinos from the Earth. However, for the case of neutrinos from the Sun, because the higher-energy neutrinos from semiprompt decays are preferentially absorbed relative to the lower-energy neutrinos coming from secondary decays [13] (such as W's decaying to pairs of quarks which subsequently decay to neutrinos), the secondary decay neutrinos may become important at large S masses. At the end of this Appendix we make an estimate of the importance of the secondary decays for the case of the Z boson final state, where it is shown that the primary decays dominate $\langle Nz^2\rangle_{Z\nu}$ ($\langle Nz^2\rangle_{Z\bar{\nu}}$) for m_S up to at least 1.4 TeV (2.2 TeV), and up to at least 860 GeV (1.3 TeV) for $\langle Nz\rangle_{Z\nu}$ ($\langle Nz\rangle_{Z\bar{\nu}}$). From the figures we see that an underestimate of the $\langle Nz^2\rangle_{Fi}$ or $\langle Nz\rangle_{Fi}$ by a factor of 2 will make very little difference to our conclusions. Thus we expect that in general our results for the case of solar S annihilations will be reliable for m_S up to at least ~1.5 TeV for the upward-moving muons and up to at least ~1 TeV for the contained events.

$SS^\dagger\to\bar{t}t,\bar{b}b$

In the case of quark final states, one must consider the details of hadronization and fragmentation of the final state quarks, which will produce hadron jets. RS [13] have used the results of the Lund Monte Carlo program, which simulates the final states of e^+e^- annihilations into fermion pairs, in order to calculate the values of $\langle Nz^2\rangle_{Fi}$ and $\langle Nz\rangle_{Fi}$ due to dark matter particles annihilating to fermion pairs. For the case of noninteracting final state quarks (appropriate for S annihilations in the Earth), one can use the RS results directly. In general, the $\langle Nz^2\rangle_{Fi}$ and $\langle Nz\rangle_{Fi}$ are given by [13]

$$\langle Nz^2\rangle_{Fi} = \frac{N}{3}\langle y^2\rangle(\langle z_F^2\rangle - \tfrac{1}{4}z_M^2) \tag{A6}$$

and

$$\langle Nz\rangle_{Fi} = \frac{N}{2}\langle y\rangle\langle z_F\rangle , \tag{A7}$$

where $z_M^2=m_H^2/m_S^2$. N, $\langle y^n\rangle$, the hadron mass m_H, and $\langle Z_F^n\rangle$ are given in Tables II and III of Ref. [13]. In this we have assumed that the mean hadron energy (scaled by the S mass) when the hadron decays, $\langle z_H\rangle$, is equal to the hadron energy after fragmentation $\langle z_F\rangle$, which is true if the hadrons are not slowed by the astrophysical medium (Sun or Earth) before they decay. We will show below that this is in general justified for the case of interest to us here. One has to correct (A6) and (A7) for the case of m_S near the threshold for producing a hadron, since in this case energy conservation implies $\langle z_F\rangle\to1$. RS make the replacement $\langle z_F^n\rangle\to\langle z_F^n\rangle+(1-\langle z_F^n\rangle)z_M^n$ in order to take this into account [13]. Using (A6) and (A7) (corrected for thresholds) and the results of Ref. [13] we obtain, for the $\bar{t}t$ final state,

$$\langle Nz^2\rangle_{t\nu_\mu} = 1.7\times10^{-2}(1-0.04z_M^2) \tag{A8}$$

and

$$\langle Nz\rangle_{t\nu_i} = 4.7\times10^{-2}(1+0.14z_M) , \tag{A9}$$

where $i=e$ or μ. The same results are obtained for the antineutrinos. For the $\bar{b}b$ final state we obtain

$$\langle Nz^2\rangle_{b\nu_\mu} = 6.5\times10^{-3}(1+0.39z_M^2) \tag{A10}$$

and

$$\langle Nz\rangle_{b\nu_i} = 2.8\times10^{-2}(1+0.41z_M) . \tag{A11}$$

These results are for the case where interactions with the astrophysical medium are ignored. For the case of solar annihilations one has to consider the possible effects of hadrons slowing before they decay, as well as the effect of neutrinos losing energy or being absorbed as they pass through the Sun. In fact, we can ignore the effect of hadrons slowing for the case of interest to us here. For the b quark final state, the effect of slowing is only important for $E_b>E_b^c=470$ GeV [13]. But the b quark final state is important only when W and Z final states are kinematically disallowed, $m_S<m_W$, in which case we can ignore the slowing of the hadrons. For the case of the t quarks, one has $E_c^t=(m_t/m_b)^{1/2}E_b^c=2.3$ TeV for $m_t=120$ GeV. For m_S large compared with m_W, the branching ratio to the W final state is much larger than that to the t quark final state. [From (2.8) we find $B_{WW}/B_{\bar{t}t}\approx2m_S^2/3m_t^2$ in the limit of large m_S.] Thus we see that for values of m_S for which slowing of the t quarks becomes important (greater than 1 TeV), we can ignore the t quark final state. Therefore in general we can ignore the effect of quarks slowing before they decay.

In order to take account of the interaction of the neutrinos with the Sun, we use the method of RS. We simply integrate the differential energy spectrum, including the P_i factors from (A5):

$$\langle Nz^n\rangle_{FiA} = \int\left[\frac{dN}{dz}\right]_{Fi}\frac{z^n dz}{(1+z/z_{Si})^{n+\alpha_i}} , \tag{A12}$$

where $z_{Si}=1/\tau_i m_S$ and $\langle Nz^n\rangle_{FiA}$ is the moment of the neutrino distribution including the effect of interactions

with the Sun. For $(n+\alpha_i)z/z_{Si}$ small compared with 1, the denominator can be expanded to give

$$\langle Nz^n\rangle_{FiA}=\langle Nz^n\rangle_{Fi}\left[1-\frac{\langle z^{n+1}\rangle}{\langle z^n\rangle}\frac{n+\alpha_i}{z_{Si}}\right]. \quad \text{(A13)}$$

Using Table 3 and Eq. (32) of [13] we find that $(\langle z\rangle,\langle z^2\rangle,\langle z^3\rangle)$ equals $(0.13,4.4\times10^{-2},2.1\times10^{-2})$ for the t quark final state and $(0.13,2.9\times10^{-2},9.5\times10^{-3})$ for the b quark final state. Thus we obtain, for the case of t final state,

$$\langle Nz^2\rangle_{t\nu_\mu A}=\langle Nz^2\rangle_{t\nu_\mu}[1-m_S/(290\text{ GeV})], \quad \text{(A14)}$$

$$\langle Nz^2\rangle_{t\bar{\nu}_\mu A}=\langle Nz^2\rangle_{t\bar{\nu}_\mu}[1-m_S/(492\text{ GeV})], \quad \text{(A15)}$$

$$\langle Nz\rangle_{t\nu_\mu A}=\langle Nz\rangle_{t\nu_\mu}[1-m_S/(478\text{ GeV})], \quad \text{(A16)}$$

$$\langle Nz\rangle_{t\bar{\nu}_\mu A}=\langle Nz\rangle_{t\bar{\nu}_\mu}[1-m_S/(765\text{ GeV})], \quad \text{(A17)}$$

and, for the b final state,

$$\langle Nz^2\rangle_{b\nu_\mu A}=\langle Nz^2\rangle_{b\nu_\mu}[1-m_S/(422\text{ GeV})], \quad \text{(A18)}$$

$$\langle Nz^2\rangle_{b\bar{\nu}_\mu A}=\langle Nz^2\rangle_{b\bar{\nu}_\mu}[1-m_S/(716\text{ GeV})], \quad \text{(A19)}$$

$$\langle Nz\rangle_{b\nu_\mu A}=\langle Nz\rangle_{b\nu_\mu}[1-m_S/(740\text{ GeV})], \quad \text{(A20)}$$

$$\langle Nz\rangle_{b\bar{\nu}_\mu A}=\langle Nz\rangle_{b\bar{\nu}_\mu}[1-m_S/(1200\text{ GeV})]. \quad \text{(A21)}$$

These should be accurate so long as the suppression factors are not too small compared to 1. However, for the case of the t quark we see that for $\langle Nz^2\rangle_{t\nu_\mu A}$ the approximation breaks down for m_S larger than about 250 GeV. In this case an alternative method for estimating the suppression of the neutrinos must be used. From Table 3 of [13] we see that the effect of fragmentation for the t quark is quite small, with $\langle z_F\rangle=0.87$ and $\langle z_F^2\rangle=0.78$, compared with 1 for the case without fragmentation. In addition, most of the neutrinos come from the primary decay mode to neutrinos, $t\to b\mu^+\nu_\mu$ [13]. This can be seen by comparing the naive estimate based on this decay mode with the results of (A8) and (A9). Assuming that in the rest frame of the decaying quark the decay is isotropic with each decay product having energy $\approx m_t/3$, the energy squared of the neutrino is $(m_S^2/9)(1+\beta^2/3)$, where $\beta=(1-m_t^2/m_S^2)^{1/2}$. The branching ratio for this t decay is $\frac{1}{9}$. Thus we obtain

$$\langle Nz^2\rangle_{t\nu_\mu}\approx(\tfrac{1}{9})^2(1+\beta^2/3)=0.012(1+\beta^2/3) \quad \text{(A22)}$$

and

$$\langle Nz\rangle_{t\nu_\mu}\approx\tfrac{1}{9}\tfrac{1}{3}=0.037, \quad \text{(A23)}$$

which in the limit $\beta\to1$ are close to (A8) and (A9).

Thus in this case a reasonable approximation to the suppression factors is to use the P_i with $E_0=m_t/3$. At large values of m_S, where such an approach may fail (due to the preferential stopping of the higher-energy primary decay neutrinos, such that the spectrum is not dominated by these neutrinos [13]), the t quark final state can be neglected compared with the gauge boson final state when calculating event rates. Thus we will use (A18)–(A21) for the b quark final state and the P_i suppression factors for the t quark final state.

$$SS^\dagger\to h^0h^0$$

RS do not explicitly discuss this case. However, we can easily adapt their results. The main decay mode of the Higgs bosons when $m_h<m_W$ (with branching ratio ≈0.9) is to $\bar{b}b$ pairs. (The Higgs boson final state can in general be neglected compared with the gauge boson final states when these are kinematically allowed.) The neutrinos occur in the decay of these $\bar{b}b$ pairs. We can simply regard the decay of the h^0h^0 pair as the injection of two $\bar{b}b$ pairs, with each b quark having a mean energy $m_S/2$. This should be a good approximation for $m_S/2\gg m_b$. In this case we can use the RS results for $\bar{b}b$ pairs, but with $m_S\to m_S/2$ and an overall factor of 2. This gives, for the noninteracting case,

$$\langle Nz^2\rangle_{h^0\nu_\mu}=3.3\times10^{-3}(1+1.6z_M^2) \quad \text{(A24)}$$

and

$$\langle Nz\rangle_{h^0\nu_i}=2.8\times10^{-2}(1+0.82z_M). \quad \text{(A25)}$$

The suppression factors for the interacting case are $[1-m_S/(844\text{ GeV})]$ (ν) and $[1-m_S/(1.4\text{ TeV})]$ $(\bar{\nu})$ for the $\langle Nz^2\rangle_{Fi}$ and $[1-m_S/(1.5\text{ TeV})]$ (ν) and $[1-m_S/(2.4\text{ TeV})]$ $(\bar{\nu})$ for the $\langle Nz\rangle_{Fi}$.

We can also use this method to estimate the contribution of the secondary decay neutrinos to the $\langle Nz^2\rangle_{Fi}$ and $\langle Nz\rangle_{Fi}$ for the case of solar S annihilations to gauge boson final states. For the case of S annihilations to a pair of Z bosons, the secondary neutrinos come from the decay of the Z's to a $\bar{b}b$, $\bar{c}c$, or $\bar{\tau}\tau$ pair. (Other lighter quark and leptons are stopped in the Sun prior to their decay and can be neglected [13].) Thus we can use the results of RS for the case of injection of a pair of b or c quarks or τ leptons each of energy $m_S/2$. (For the b and c quarks, this will overestimate the contribution when $m_S/2>E_b^c$ or E_c^c, since we are then neglecting the slowing of the b and c quarks prior to their decay.) The branching ratio for Z decay is 0.15 to a b quark pair, 0.12 to a c quark pair, and 0.033 to a τ lepton pair [19]. Thus we find, using the results of RS, that the contribution of the secondary decays is given by

$$\langle Nz^2\rangle_{Zb\nu}\approx4.9\times10^{-4}, \quad \text{(A26a)}$$

$$\langle Nz^2\rangle_{Zc\nu}\approx1.7\times10^{-4}, \quad \text{(A26b)}$$

$$\langle Nz^2\rangle_{Z\tau\nu}\approx3.8\times10^{-4}, \quad \text{(A26c)}$$

and

$$\langle Nz\rangle_{Zb\nu}\approx4.2\times10^{-3}, \quad \text{(A27a)}$$

$$\langle Nz\rangle_{Zc\nu}\approx1.4\times10^{-3}, \quad \text{(A27b)}$$

$$\langle Nz\rangle_{Z\tau\nu}\approx1.7\times10^{-3}, \quad \text{(A27c)}$$

where, for example, $\langle Nz^n \rangle_{Zb\nu}$ denotes the unsuppressed contribution coming from Z decays to b quark pairs. Comparing with the primary Z decays, we find that the unsuppressed primary decay contribution to $\langle Nz^2 \rangle_{Fi}$ is about 45 times the secondary contribution, and that the unsuppressed primary decay contribution to $\langle Nz \rangle_{Fi}$ is about nine times the secondary contribution. Thus, ignoring suppression of the secondary neutrinos, we find from (A5) that the primary and secondary decay neutrino contributions become comparable at $m_S \approx 1.4$ TeV for $\langle Nz^2 \rangle_{Z\nu}$, $m_S \approx 2.2$ TeV for $\langle Nz^2 \rangle_{Z\bar{\nu}}$, $m_S \approx 860$ GeV for $\langle Nz \rangle_{Z\nu}$, and $m_S \approx 1.3$ TeV for $\langle Nz \rangle_{Z\bar{\nu}}$.

[1] E. W. Kolb and M. S. Turner, *The Early Universe* (Addison-Wesley, Reading, MA, 1990).

[2] A. Dekel, S. M. Faber, and M. Davis, in *From the Planck Scale to the Weak Scale,* Proceedings of the Conference, Santa Cruz, California, 1987, edited by H. Haber (World Scientific, Singapore, 1987), Vol. 2; M. S. Turner, "Dark Matter in the Universe," Fermilab Report No. FERMILAB-Conf-91/78-A (unpublished).

[3] J. Yang, M. S. Turner, G. Steigman, D. N. Schramm, and K. A. Olive, Astrophys. J. **281**, 493 (1984); K. A. Olive, D. N. Schramm, G. Steigman, and T. P. Walker, Phys. Lett. B **236**, 454 (1990); T. P. Walker, G. Steigman, D. N. Schramm, K. A. Olive, and H. S. Kang, Astrophys. J. **376**, 51 (1991).

[4] A. Guth, Phys. Rev. D **23**, 347 (1981).

[5] G. R. Blumental, S. M. Faber, J. R. Primack, and M. Rees, Nature (London) **311**, 517 (1984).

[6] G. F. Smoot *et al.*, Astrophys. J. **396**, L1 (1992); E. L. Wright *et al.*, *ibid.* **396**, L13 (1992).

[7] D. Hegyi and K. A. Olive, Phys. Lett. **126B**, 28 (1983); Astrophys. J. **303**, 56 (1986); D. Ryu, K. A. Olive, and J. Silk, *ibid.* **353**, 81 (1990).

[8] D. Richstone, A. Gould, P. Guhathakurta, and C. Flynn, Astrophys. J. **388**, 354 (1992); H. B. Richer and G. G. Fahlman, Nature (London) **358**, 383 (1992).

[9] C. Alcock *et al.*, Nature (London) **365**, 621 (1993); E. Aubourg *et al.*, *ibid.* **365**, 623 (1993).

[10] S. P. Ahlen *et al.*, Phys. Lett. B **195**, 603 (1987); D. O. Caldwell *et al.*, Phys. Rev. Lett. **61**, 510 (1988); **65**, 1305 (1990).

[11] D. O. Caldwell, in *Neutrino '92,* Proceedings of the XVth International Conference on Neutrino Physics and Astrophysics, Granada, Spain, 1992, edited by A. Morales [Nucl. Phys. B (Proc. Suppl) **31**, 371 (1983)].

[12] W. H. Press and D. Spergel, Astrophys. J. **296**, 679 (1985); K. Greist and D. Seckel, Nucl. Phys. **B283**, 681 (1987); **B296**, 1034(E) (1988).

[13] S. Ritz and D. Seckel, Nucl. Phys. **B304**, 877 (1988).

[14] A. Gould, Astrophys. J. **321**, 571 (1987); **368**, 610 (1991); **388**, 338 (1992).

[15] A. Gould, Astrophys. J. **387**, 21 (1992).

[16] M. Kamionkowski, Phys. Rev. D **44**, 3021 (1991).

[17] G. B. Gelmini, P. Gondolo, and E. Roulet, Nucl. Phys. **B351**, 623 (1991).

[18] B. W. Lee and S. Weinberg, Phys. Rev. Lett. **39**, 165 (1977).

[19] V. D. Barger and R. J. N. Phillips, *Collider Physics* (Addison-Wesley, Reading, MA, 1987).

[20] G. W. Anderson and L. J. Hall, Phys. Rev. D **42**, 2685 (1992).

[21] M. A. Shifman, A. I. Vainstein, and V. I. Zahkarov, Phys. Lett. **78B**, 443 (1978); T. P. Cheng, Phys. Rev. D **38**, 2869 (1988); H. Y. Cheng, Phys. Lett. B **219**, 347 (1989); R. Barbieri, M. Frigeni, and G. F. Giudice, Nucl. Phys. **B313**, 725 (1989).

[22] J. Ellis and R. A. Flores, Phys. Lett. B **263**, 259 (1991).

[23] K. Freese, J. Frieman, and A. Gould, Phys. Rev. D **37**, 3388 (1988); K. Greist, *ibid.* **38**, 2357 (1988).

[24] P. F. Smith and J. D. Lewin, Phys. Rep. **187**, 203 (1990); P. F. Smith *et al.*, Phys. Lett. B **255**, 451 (1991).

[25] B. Cabrera, in Proceedings of the IFT Conference on Dark Matter, Gainesville, Florida, 1992 (unpublished); J. Ellis and R. A. Flores, Phys. Lett. B **300**, 175 (1993).

[26] IMB Collaboration, J. M. LoSecco *et al.*, Phys. Lett. B **188**, 388 (1987); R. Svoboda *et al.*, Astrophys. J. **315**, 420 (1987).

[27] F. Halzen, T. Stelzer, and M. Kamionkowski, Phys. Rev. D **45**, 4439 (1992).

[28] R. C. Webb, in *Proceedings of the International School of Astroparticle Physics,* The Woodlands, Texas, 1991, edited by D. V. Nanopoulos (World Scientific, Singapore, 1993).

[29] A. Okada *et al.*, in *Proceedings of the Workshop on High Energy Neutrino Astrophysics,* Honolulu, Hawaii, 1992, edited by V. J. Stenger *et al.* (World Scientific, Singapore, 1992); DUMAND Collaboration, Phys. Rev. D **42**, 3613 (1990).

[30] S. Tilev *et al.*, in *Proceedings of the 23rd International Cosmic Ray Conference,* Calgary, Canada, 1993, edited by D. A. Leahy (University of Calgary, Calgary, 1993).

[31] *Proceedings of the NESTOR Workshop,* Pylos, Greece, 1992, edited by L. K. Resvanis (University of Athens, Athens, 1993); L. K. Resvanis, Europhys. News **23**, 172 (1992).

[32] F. Halzen and J G. Learned, University of Wisconsin-Madison Report No. MAD/PH/759, 1993 (unpublished); J. G. Learned, in *Neutrino '92* [11], p. 456.

[33] Frejus Collaboration, H. J. Daum, in *Astrophysics and Particle Physics,* Proceedings of the Topical Seminar, San-Miniato, Italy, 1989, edited by G. Castellini *et al.* [Nucl. Phys. B (Proc. Suppl.) **14B** (1990)].